2D Conducting Polymers

International Edition: DOI: 10.1002/anie.201503332
German Edition: DOI: 10.1002/ange.201503332

High-Conductivity Two-Dimensional Polyaniline Nanosheets Developed on Ice Surfaces**

*Il Young Choi, Joungphil Lee, Hyungmin Ahn, Jinho Lee, Hee Cheul Choi, and Moon Jeong Park**

Abstract: *A new method to develop two-dimensional PANI nanosheets using ice as a removable hard template is presented. Distinctly high current flows of 5.5 mA at 1 V and a high electrical conductivity of 35 S cm^{-1} were obtained for the polyaniline (PANI) nanosheets, which marked a significant improvement from previously values on other PANIs reported over the past decades. These improved electrical properties of ice-templated PANI nanosheets were attributed to the long-range ordered edge-on π-stacking of the quinoid ring, ascribed to the ice surface-assisted vertical growth of PANI. The unprecedented advantages of the ice-templated PANI nanosheets are two-fold. First, the PANI nanosheet can be easily transferred onto various types of substrates via float-off from the ice surfaces. Second, PANI can be patterned into any shape using predetermined masks, and this is expected to facilitate the eventual convenient and inexpensive application of conducting polymers in versatile electronic device forms.*

Since the discovery of conducting polymers in the mid-19th century,[1] considerable efforts have been devoted, particularly over the past few decades, on their practical applications in a range of electronic devices, such as thin-film transistors,[2] light emitting diodes,[3] solar cells,[4] batteries,[5] and supercapacitors.[6] In particular, much of the research has focused on exploiting methods for the synthesis of conducting polymers to improve their electrical properties and processability. Examples of conducting polymers with established synthetic procedures include polyaniline (PANI),[3,7] polypyrrole (PPy),[5,8] poly(*p*-phenylene vinylene) (PPV),[9] and poly(thiophene) (PT) derivatives.[2]

Among a variety of conducting polymers, PANI has long been considered a promising candidate for microelectronics and battery electrodes because of its high electrical conductivity, facile wet chemical synthesis at low cost, easy doping process, and good environmental stability.[10] PANI in the emeraldine salt form demonstrated a high electrical conductivity ranging from 10^{-3} to 10^{2} S cm^{-1} with varying conjugation length,[11] doping level,[12] and the type of dopant.[13] Decades of research on PANI have further revealed that the electrical properties of PANI can be largely tailored by changing the dimensionality of nanostructures.[14]

As an efficient approach to produce different PANI nanostructures, templated synthesis has widely been employed, which can be classified as follows: 1) synthesis using structured hard templates to direct the growth of aniline;[15] and 2) a soft template route via oxidative polymerization of aniline.[16] Various PANI structures such as nanoparticles,[17] nanotubes,[18] nanofibers,[10,19] nanowires,[20] nanosheets,[21] and networks[3,22] have been prepared by employing hard and soft templates that have stimulated investigations of the structure–property relationship of PANI. The results emphasized the importance of developing two-dimensional (2D) morphologies to achieve enhanced electrical properties, especially in desired directions, to realize their applications in high-density integrated electronic devices.[14,23]

Successful fabrication of 2D PANI nanostructures previously reported have mostly relied on the use of graphene oxide (GO) as a hard template[6,24] because of its 2D nature in terms of atomic thickness and high surface area. In particular, the oxygen groups in GO serve as active sites capable of hydrogen bonding with aniline to facilitate 2D growth of aniline along basal plane of GO via π–π stacking interactions.[25] This resulted in the so-called PANI/GO composite nanosheets, which showed improved electrical properties and high mechanical strength.[26] While the results are promising, GO is likely to yield an inhomogeneous distribution and irreversible agglomerates, causing difficulty in obtaining reliable electrical properties over a large area.[27] High cost, complicated synthetic procedures, and difficulty in removal of the GO template are also fundamental shortcomings of the PANI/GO composites. This suggested the necessity of developing new technologies to prepare pure 2D PANI nanostructures over a large area as a novel prospect for next generation electronic devices, but it remains a challenging task yet because of the difficulties in controlling surface and interfacial properties.

Herein, we present a facile synthesis of pure 2D PANI nanosheets a few millimeters in diameter with improved electronic properties via chemical oxidative polymerization. The key to success stemmed from the use of ice as a new type of hard template, providing the unique surface of water molecules with lower potential energy than bulk water. The easy removal of ice also enabled the attainment of template-

[*] I. Y. Choi,[+] J. Lee,[+] H. Ahn, Prof. M. J. Park
Department of Chemistry, Division of Advanced Materials Science
Pohang University of Science and Technology (POSTECH)
Pohang 790-784 (Korea)
E-mail: moonpark@postech.edu
J. Lee, Prof. H. C. Choi
Center for Artificial Low Dimensional Electronic Systems, Institute for Basic Science (Korea)
[+] These authors contributed equally to this work.

[**] This work was supported by the Samsung Research Funding Center of Samsung Electronics under Project Number SRFC-MA1402-08.
Supporting information for this article is available on the WWW under http://dx.doi.org/10.1002/anie.201503332.

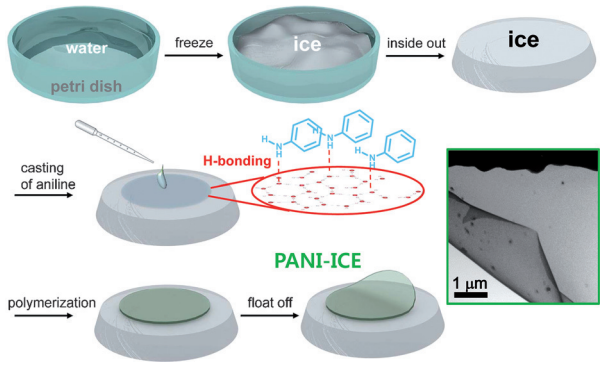

Scheme 1. Illustration of the synthetic procedures for 2D PANI nanosheets on ice surfaces (PANI-ICE). Inset: TEM micrograph confirming the formation of 2D nanosheet with few defects.

free PANI nanosheets with a thickness of tens of nanometers, through a simple melting process.

Scheme 1 depicts the synthetic procedures for the 2D PANI nanosheets on the ice surface (hereafter, referred to as PANI-ICE). First, aniline solution in 1 M HCl was cast on the ice frozen in a petri dish, which provides a smooth surface after turning it upside down. Ammonium peroxydisulfate solution in 1 M HCl was then immediately added dropwise on the ice with the aniline deposit to allow chemical oxidation of aniline monomers while the reaction temperature was kept stable at 0 °C. The protonated anilinium can be readily adsorbed on the dangling OH groups at the ice surfaces by hydrogen bonding and electrostatic interactions (Supporting Information, Figure S1). Note that the presence of aniline prevents the ice surface from melting by HCl owing to the limited extent of proton transfer from HCl to the ice.[28] The use of deep frozen ice at −20 °C also plays an important role in retarding the etching of the ice surface. Upon oxidative polymerization for 3 min, the formation of PANI-ICE a few millimeters in diameter becomes apparent to the naked eye. The thickness of PANI-ICE was ca. 30 nm, as measured by a scanning probe microscope after transferring the sample onto the Si/SiO_2 substrate. The formation of 2D nanosheets with few defects was confirmed by transmission electron microscopy (TEM), as shown in the inset. Considering the fact that most reports on chemical oxidative polymerization of PANI have 0D[17] or 1D PANI morphologies[18] that are ascribed to surface-induced aggregation, the facile fabrication of a 2D PANI nanostructure simply by introducing ice templates is noteworthy.

To study the synthesis mechanisms of PANI-ICE, PANI on the ice surface was monitored in situ using an optical microscope equipped with cryogenic sample stages. Photographs of PANI-ICE intermediates taken during the middle of the reaction are shown in Figure 1 a. We see the intriguing appearance of a uniform layer of aniline with a diameter of several millimeters in the early stage of the reaction (< 30 s), ascribed to the readily adsorbed nuclei or oligomers via hydrogen bonding interaction. The lower potential energy of ice at the PANI/ice interfaces compared to that of bulk water should also play a key role in developing large-area wetting layer of aniline by reducing nucleation barrier.[29] As the

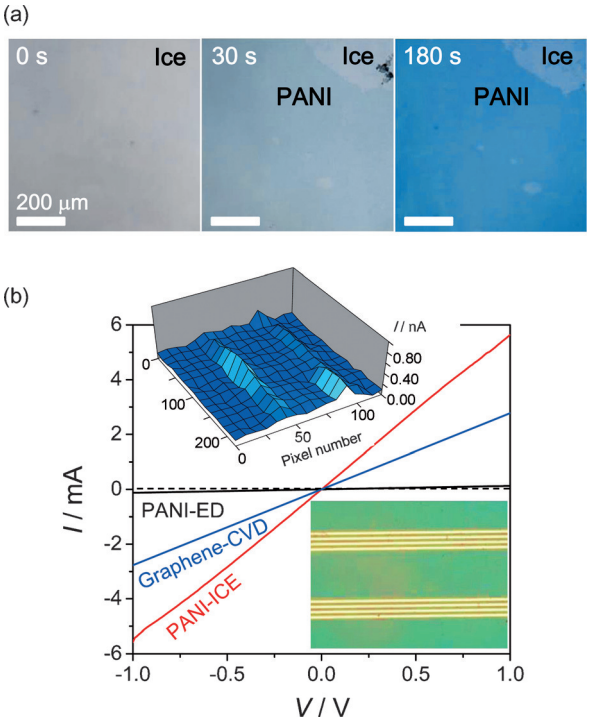

Figure 1. a) In situ imaging of the synthesis of PANI on ice surfaces, where photographs were taken during the middle of the reaction, as noted in the figure. b) *I–V* characteristic curve of PANI-ICE, compared to those of PANI-ED and graphene-CVD. Inset: Optical micrograph of PANI-ICE on gold electrodes.

oxidation reaction proceeds, no significant change in the size of nanosheets was noticed, but preferential vertical growth of PANI was perceived through the increasingly dark blue color, eventually yielding uniform large-area PANI nanosheets within 3 min of the reaction.

We first investigated the electrical properties of PANI-ICE by measuring current-voltage (*I–V*) characteristics by sweeping voltages between −1.0 and 1.0 V at constant temperature and humidity conditions (25 °C and 20 %). Figure 1 b shows representative *I–V* curves of PANI-ICE compared to that of conventional PANI thin films prepared by galvanostatic electrochemical deposition method (referred to as PANI-ED), measured using gold electrodes (10 μm wide and 10 μm apart) on Si/SiO_2 substrates (see inset photograph showing PANI-ICE placed on top of the gold electrodes). Interestingly, a distinctly high current flow of 5.5 mA at 1 V was obtained for PANI-ICE with linear *I–V* characteristics, contrary to a low current flow of 0.12 mA for PANI-ED. The uniformity of PANI-ICE in the entire area was further confirmed by a spatially resolved photocurrent imaging technique using a focused laser beam with 500 nm diameter and 532 nm wavelength under 0.1 V bias. A representative result acquired over an area of 30 × 30 μm is given in the inset.

By taking into account the size and thickness of each sample, the electrical conductivities of PANI-ICE and PANI-ED were calculated using the equation:

$$\sigma = \frac{L \cdot I}{V \cdot A}$$

where L is the distance between gold electrodes (10 μm), I is the electric current, V is the applied voltage, and A is the cross-sectional area of the sample. Notably, electrical conductivity of PANI-ICE was determined to be 35 $S\,cm^{-1}$, which is two orders of magnitude higher than that of PANI-ED (0.8 $S\,cm^{-1}$). To the best of our knowledge, we report the highest electrical conductivity for PANI as compared to the values of any other PANIs reported in the literature (by focusing on the use of HCl as the most common doping agent), which are typically around 1 $S\,cm^{-1}$, analogous to our PANI-ED. This clearly indicates the impact of our results on the structure of conducting polymers based on PANI. It should be noted that the electrical properties of PANI-ICE were largely depending on the synthesis temperature, where three orders of magnitude lower current flows were attained at subzero temperature conditions (Supporting Information, Figure S2). This can be rationalized by the formation of heterogeneous nuclei and agglomerates.[30] The I–V curve of graphene synthesized by chemical vapor deposition (graphene-CVD, sheet resistance of ca. 360 $ohm\,sq^{-1}$, Raman spectrum is given in the Supporting Information, Figure S3) is also shown in Figure 1 b as a benchmark material, suggesting that our PANI-ICE can serve as a new electrical soft material with superior electrical properties. The additional benefits of fast and large-area synthesis at low cost for our PANI-ICE are worth noting.

Because it is well-known that the key parameters affecting electrical conductivities of conducting polymers are conjugation length[11] and doping level,[12] molecular characteristics of PANI-ICE were examined in comparison to PANI-ED. As shown in the Supporting Information, Figure S4, from the UV/Vis and IR absorption spectra, essentially the same conjugation length and doping level were identified for PANI-ICE and PANI-ED. We thus deduce that the improvement in the electrical conductivity of PANI-ICE did not originate from chemical factors.

Mechanisms underlying the improved electrical properties could be ascribed to the intriguing molecular orientation and high crystallinity of PANI-ICE. The structural characteristics of PANI-ICE were studied using X-ray powder diffraction (XRD) and selected area electron diffraction (SAED) in TEM. The XRD profile was obtained from a number of ground pieces of PANI-ICEs to achieve enough scattering intensities, which indicated that aniline molecules assembled in PANI-ICE have a long-range order with an orthorhombic $P222$ space group, as indexed in Figure 2 a, with the unit cell parameters of $a = 17.356$ Å, $b = 7.012$ Å, $c = 8.579$ Å, and $\alpha = \beta = \gamma = 90.00°$. It is thus inferred that PANI molecules are π–π stacked along the b-axis with a d spacing of ca. 3.51 Å and the PANI main chains are periodically positioned with a d spacing of ca. 4.29 Å along the d-axis. The average crystallite size of PANI-ICE is estimated to be large as 68 ± 4 nm from the XRD profile using the Scherrer equation (a shape factor of 1 was used).[31] From SAED, the quinoid rings in PANI-ICE are predominantly found to be tiled in the vertical direction over the entire area examined. A representative result is given in Figure 2 b, where the brightest (020) reflection of PANI-ICE indicated an edge-on π–π stacking of conjugated rings, as illustrated in Figure 2 c. A SAED pattern taken along [011] direction is also provided in the Supporting Information, Figure S5.

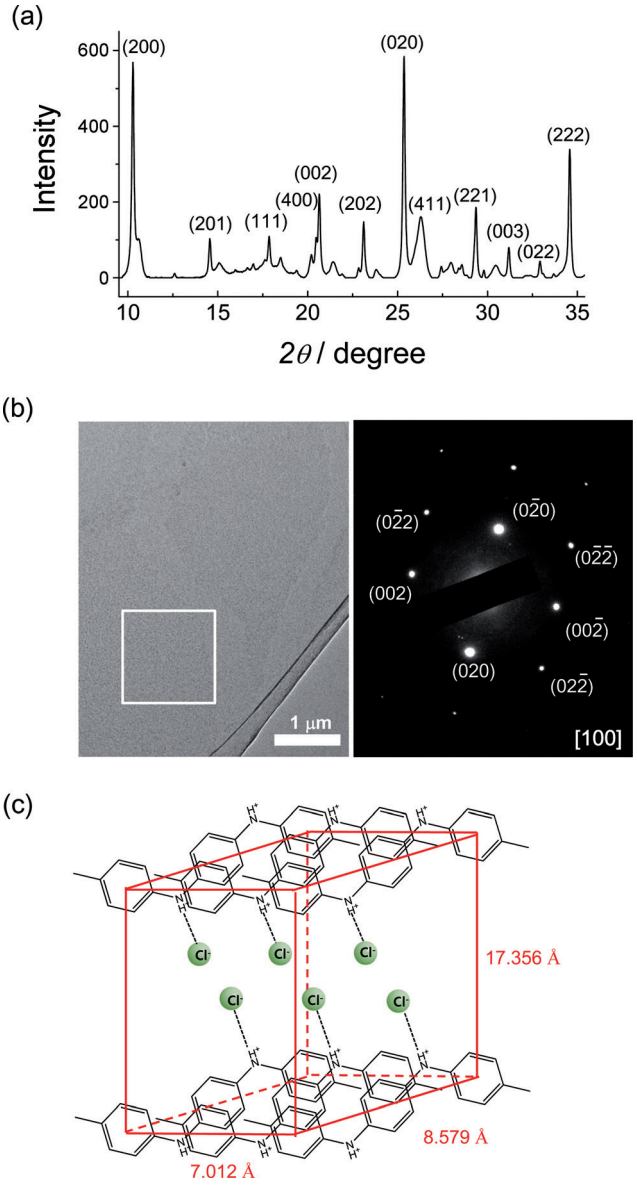

Figure 2. The structural characteristics of PANI-ICE determined by combining a) X-ray powder diffraction and b) selected-area electron-diffraction that indicate highly crystalline PANI-ICE with an orthorhombic structure, as indexed in (a) and (b). c) Representation of the determined orthorhombic structure with an edge-on π–π stacking of conjugated rings for PANI-ICE.

This implies that the ice surface influenced the packing properties of aniline molecules in developing long-range ordered 2D nanostructures, intimately associated with the improved electrical conductivity. To further support our hypothesis, we have synthesized 2D PANI nanosheets on different OH-containing substrates, that is, Si-wafer and glass, under the same synthetic conditions. Interestingly, the resulting PANI nanosheets appeared to be very defective and porous, leading to a current flow that is a few orders of magnitude lower (see I–V curve and optical micrograph of PANI synthesized on glass substrate in the Supporting

Information, Figure S6). This is due to the formation of heterogeneous nuclei and aggregation under the low temperature conditions, consistent with previous reports,[30] but the same analogy could not be found in PANI-ICE. It should be noted that when the synthesis of PANI on glass was monitored in situ (Supporting Information, Figure S7), nucleation of PANI with an average size of a few micrometers was readily detected in the early stages of the reaction, followed by the common nucleation and growth mechanisms to coalesce into large PANI aggregates with time.[32] This clearly indicated the importance of ice surfaces with the layer of quasi-ordered water molecules in forming uniform and large-area 2D PANI nanosheets.

The unprecedented advantages of PANI-ICE compared to other reported conducting polymers are as follows. First of all, on account of easy removal of the ice-template, PANI-ICE is transferable onto any kind of substrate such as metals, indium tin oxide (ITO), Si-wafer, glass, and even polymer substrates, which have not been reported previously. The photographs of PANI-ICE on different substrates are given in Figure 3a. Furthermore, micropatterned PANI can be easily

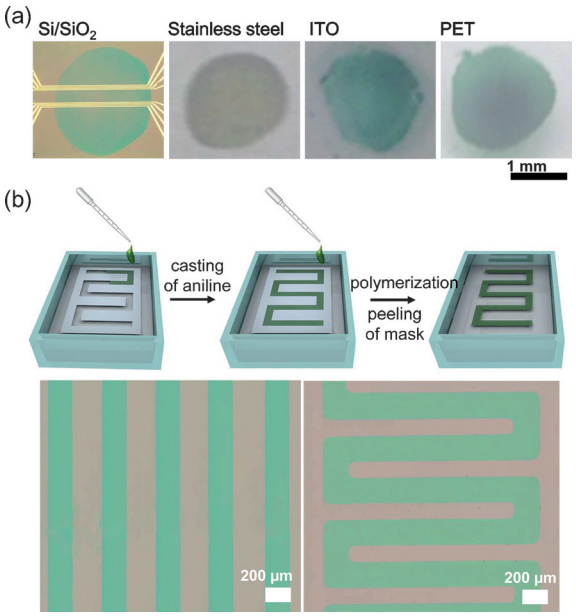

Figure 3. a) Photographs of transferred PANI-ICE onto different substrates as noted by float-off from ice surfaces. (b) Optical micrographs of micropatterned PANI-ICE into parallel lines and periodic lines with 90° bends using metal masks.

prepared using micropatterned masks. As representative examples, optical micrographs of patterned PANI-ICE into parallel lines and periodic lines with 90° bends are shown in Figure 3b. In principle, it can be patterned into any shape with predetermined masks, suggesting new avenues towards future organic electronics technologies. Experiments on the small pitch sizes will be a subject of our future studies.

In summary, a facile synthesis of highly conducting 2D PANI nanosheets by chemical oxidative polymerization was investigated in this study. The ice-templated PANI nanosheet demonstrated electrical conductivity that was a few orders of magnitude higher than that of most HCl-doped PANIs reported to date. This is ascribed to the unique advantage of ice surfaces, offering low potential energy and quasi-ordered dangling OH groups. To the best of our knowledge, this work demonstrates the first example of patternable, transferable, and pure 2D conducting polymers with advanced electrical properties.

Experimental Section

PANI-ICE was synthesized by chemical oxidation polymerization on ice surfaces at 0°C using aniline (>99.5%, Sigma–Aldrich) and ammonium peroxydisulfate (APS) (>98.0%, Alfa Aesar). Water was frozen at −20°C in a petri dish, which was flipped over for the synthesis to provide a smooth surface. Aniline (0.25 M in 1 M HCl) and APS (0.25 M in 1 M HCl) were employed, where the molar ratio of aniline to APS was 8:3. After 3 min of reaction, the formation of 2D nanosheets with a diameter of a few millimeters was apparent to the naked eye. After transferring PANI-ICE onto the Si-wafer via float-off from the ice surface, the PANI-ICE was washed repeatedly with deionized water and dried in a vacuum oven for a week.

Morphology and molecular orientation of PANI-ICE were investigated by transmission electron microscopy (JEOL-JEM-2100F) equipped with selected area electron diffraction. The crystal structure of PANI was characterized by powder X-ray diffraction. The diffraction data were collected in a 2D beamline at the Pohang Accelerator Laboratory using synchrotron radiation. In situ monitoring of the synthesis of PANI-ICE was performed using an optical microscope (RMC Ultramicrotome) equipped with cryogenic sample stages. *I–V* curves of PANI-ICE were measured using a semiconductor analyzer (Keithley 4200) at 25°C and RH = 20%. Data were collected over a voltage range of −1.0 to 1.0 V using the linear sweep mode. Spatially resolved photocurrents were acquired using a focused laser beam of 500 nm in diameter at 532 nm wavelength under a 0.1 V bias.

Keywords: conducting materials · ice surfaces · micropatterns · nanostructures · polymers

How to cite: *Angew. Chem. Int. Ed.* **2015**, *54*, 10497–10501
Angew. Chem. **2015**, *127*, 10643–10647

[1] H. Letheby, *J. Chem. Soc.* **1862**, *15*, 161–163.
[2] H. Klauk, *Chem. Soc. Rev.* **2010**, *39*, 2643–2666.
[3] Y. Yang, E. Westerweele, C. Zhang, P. Smith, A. J. Heeger, *J. Appl. Phys.* **1995**, *77*, 694–698.
[4] J. Y. Kim, K. Lee, N. E. Coates, D. Moses, T. Nguyen, M. Dante, A. J. Heeger, *Science* **2007**, *317*, 222–225.
[5] H.-K. Song, G. T. R. Palmore, *Adv. Mater.* **2006**, *18*, 1764–1768.
[6] Q, Wu, Y. Xu, Z. Yao, A. Liu, G. Shi, *ACS Nano* **2010**, *4*, 1963–1970.
[7] N. Toshima, S. Hara, *Prog. Polym. Sci.* **1995**, *20*, 155–183.
[8] C. Jérôme, R. Jérôme, *Angew. Chem. Int. Ed.* **1998**, *37*, 2488–2490; *Angew. Chem.* **1998**, *110*, 2639–2642.
[9] N. D. Kumar, J. D. Bhawalkar, P. N. Prasad, F. E. Karasz, B. Hu, *Appl. Phys. Lett.* **1997**, *71*, 999–1001.
[10] a) J. Huang, S. Virji, B. H. Weiller, R. B. Kaner, *J. Am. Chem. Soc.* **2003**, *125*, 314–315; b) X. S. Du, C. F. Zhou, Y. W. Mai, *J. Phys. Chem. C* **2008**, *112*, 19836–19840; c) H. Zhang, X. Wang, J. Li, F. Wang, *Synth. Met.* **2009**, *159*, 1508–1511.
[11] Y. Yang, S. Chen, L. Xu, *Macromol. Rapid Commun.* **2011**, *32*, 593–597.
[12] J. Jin, Q. Wang, M. A. Haque, *J. Phys. D* **2010**, *43*, 205302–205306.

[13] J. Stejskal, D. Hlavatá, P. Holler, M. Trchová, J. ProkeŠ, I. Sapurina, *Polym. Int.* **2004**, *53*, 294 – 300.
[14] Y. Wang, H. D. Tran, L. Liao, X. Duan, R. B. Kaner, *J. Am. Chem. Soc.* **2010**, *132*, 10365 – 10373.
[15] a) C. G. Wu, T. Bein, *Science* **1994**, *264*, 1757 – 1759; b) C. R. Martin, *Acc. Chem. Res.* **1995**, *28*, 61 – 68.
[16] a) J. Ryu, C. B. Park, *Angew. Chem. Int. Ed.* **2009**, *48*, 4820 – 4823; *Angew. Chem.* **2009**, *121*, 4914 – 4917; b) L. Zhang, M. Wan, *Adv. Funct. Mater.* **2003**, *13*, 815 – 820.
[17] a) H. Gao, T. Jiang, B. Han, Y. Wang, J. Du, Z. Liu, J. Zhang, *Polymer* **2004**, *45*, 3017 – 3019; b) G. M. Neelgund, A. Oki, *Polym. Int.* **2011**, *60*, 1291 – 1295.
[18] a) Y. Long, Z. Chen, N. Wang, Y. Ma, Z. Zhang, L. Zhang, M. Wan, *Appl. Phys. Lett.* **2003**, *83*, 1863 – 1865; b) H. Ding, J. Shen, M. Wan, Z. Chen, *Macromol. Chem. Phys.* **2008**, *209*, 864 – 871; c) W. Chen, R. B. Rakhi, H. N. Alshareef, *J. Mater. Chem. A* **2013**, *1*, 3315 – 3324.
[19] a) X. Zhang, W. J. Goux, S. K. Manohar, *J. Am. Chem. Soc.* **2004**, *126*, 4502 – 4503; b) J. Huang, R. B. Kaner, *J. Am. Chem. Soc.* **2004**, *126*, 851 – 855; c) J. Huang, R. B. Kaner, *Angew. Chem. Int. Ed.* **2004**, *43*, 5817 – 5821; *Angew. Chem.* **2004**, *116*, 5941 – 5945.
[20] a) H. Qiu, J. Zhai, S. Li, L. Jiang, M. Wan, *Adv. Funct. Mater.* **2003**, *13*, 925 – 928; b) J. Xu, K. Wang, S. Z. Zu, B. H. Han, Z. Wei, *ACS Nano* **2010**, *4*, 5019 – 5026; c) K. Wang, Q. Meng, Y. Zhang, Z. Wei, M. Miao, *Adv. Mater.* **2013**, *25*, 1494 – 1498.
[21] a) X. Zhou, T. Wu, B. Hu, G. Yang, B. Han, *Chem. Commun.* **2010**, *46*, 3663 – 3665; b) Y. Zhang, X. Zhuang, Y. Su, F. Zhang, X. Feng, *J. Mater. Chem. A* **2014**, *2*, 7742 – 7746.
[22] a) Y. Zhu, H. He, M. Wan, L. Jiang, *Macromol. Rapid Commun.* **2008**, *29*, 1705 – 1710; b) S. Jafarzadeh, P. Claesson, P.-E. Sundell, J. Pan, E. Thormann, *ACS Appl. Mater. Interfaces* **2014**, *6*, 19168 – 19175.
[23] a) Z. Wei, T. Laitinen, B. Smarsly, O. Ikkala, C. F. J. Faul, *Angew. Chem. Int. Ed.* **2005**, *44*, 751 – 756; *Angew. Chem.* **2005**, *117*, 761 – 766; b) Y. Yan, J. Fang, Y. Zhang, H. Fan, Z. Wei, *Macromol. Rapid Commun.* **2011**, *32*, 1640 – 1644; c) S. Li, D. Wu, C. Cheng, J. Wang, F. Zhang, Y. Su, X. Feng, *Angew. Chem. Int. Ed.* **2013**, *52*, 12105 – 12109; *Angew. Chem.* **2013**, *125*, 12327 – 12331.
[24] a) D. W. Wang, F. Li, J. Zhao, W. Ren, Z. G. Chen, J. Tan, Z. S. Wu, I. Gentle, G. Q. Lu, H. M. Cheng, *ACS Nano* **2009**, *3*, 1745 – 1752; b) H. Wang, Q. Hao, X. Yang, L. Lu, X. Wang, *ACS Appl. Mater. Interfaces* **2010**, *2*, 821 – 828.
[25] Y. Liu, R. Deng, Z. Wang, H. Liu, *J. Mater. Chem.* **2012**, *22*, 13619 – 13624.
[26] W. Fan, Y.-E. Miao, L. Zhang, Y. Huang, T. Liu, *RSC Adv.* **2015**, *5*, 31064 – 31073.
[27] N.-R. Chiou, C. Lu, J. Guan, J. Lee, A. J. Epstein, *Nat. Nanotechnol.* **2007**, *2*, 354 – 357.
[28] S.-C. Park, K.-W. Maeng, T. Pradeep, H. Kang, *Angew. Chem. Int. Ed.* **2001**, *40*, 1497 – 1500; *Angew. Chem.* **2001**, *113*, 1545 – 1548.
[29] P. Pirzadeh, P. G. Kusalik, *J. Am. Chem. Soc.* **2013**, *135*, 7278 – 7287.
[30] N. Joseph, J. Varghese, M. T. Sebastian, *RSC Adv.* **2015**, *5*, 20459 – 20466.
[31] A. L. Patterson, *Phys. Rev.* **1939**, *56*, 978 – 982.
[32] N. T. Kemp, J. W. Cochrane, R. Newbury, *Synth. Met.* **2009**, *159*, 435 – 444.

Received: April 13, 2015
Revised: May 8, 2015
Published online: June 18, 2015

